File: `c:\filter\causal_acausal_low_cut_filters.tex`

Some notes on processing: causal vs. acausal low-cut filters
version 1.0

David M. Boore

Introduction

These are some informal notes showing results of some procedures used in the processing of strong-motion data. Most of these informal notes are devoted to a comparison of causal and acausal low-cut[†] filtering. I show that causally-filtered records can be sensitive to the cutoff period of the filter even for oscillator periods much shorter than the filter cutoff periods. Boore and Akkar (2003) found this to be particularly noticeable for inelastic spectra, but new to this note is the finding that peak accelerations can be sensitive to the long-period cutoffs. These findings lead me to the conclusion that acausal filters should be used in processing. This may be of interest to the PEER NGA database effort, because the PEER database has been processed using causal low-cut filters (from 1999 until recently, the USGS also used causal filters).

I also show one comparison of response spectra computed for causally-filtered accelerations with and without the trailing filter transients (neither the USGS or PEER include the trailing filter transient in their computations of response spectra). The comparison suggests that the effect of not including the transient is only important for oscillator periods in larger than about 30 sec.

Finally, I offer a few comments about the useable frequency range of filtered records. If the displacements based on double integration of the acceleration time series reach a relatively constant level at the end of the record (this can be achieved using baseline corrections), then a low-order filter is sufficient to remove the long-period noise (whether causal or acausal, we generally use a filter whose response goes as f^4 at low frequencies). The lower the order of the filter, the less the ringing associated with the filter cutoff. On the other hand, by definition the low-order filters are less sharp than higher-order filters, requiring a broader

---

[†] Although EEs seem to like the term "high-pass", I prefer "low-cut" because it describes the active part of what the filter does: it cuts out the low frequencies (the active role of a filter), allowing the high frequencies to pass (the passive role of a filter).

– 1 –

transition band in the frequency domain. This leads to the rule-of-thumb that response spectra of filtered records should be used for oscillator periods less than about 0.5 the filter corner frequency if low-order filters are used; this is more restrictive than recommended by other groups, who may use filters with transitions over narrower frequency ranges.

In the interests of getting these results into circulation in a timely manner, the text is very brief. This report is primarily consists of a number of tables and figures showing the results of processing. I hope that the reader will spend time studying the tables and figures.

Unless noted, all filtering, integration, and computation were done using my software, which can be obtained from the online software link on my web page (`http://quake.usgs.gov/~boore`).

<div align="center">Properties of causal and acausal filters</div>

Before showing the results, a short discussion of the properties of causal and acausal filters is in order. The filters used here are Butterworth filters implemented in the time-domain. Acausal filtering is done by running a time-domain causal filter forwards and backwards through the time series, with the number of poles of the causal filter chosen so that the filter responses of both the causally and acausally filtered data are the same at long periods (in my examples the long-period responses go as T^{-4}). The time-domain impulse responses and the amplitude and phase spectra are shown in Figure 1 for most of the filters considered in these notes. The essential difference in the filters is that the causal filter will produce no precursory motion when applied to a time series, but this comes at the expense of a significant distortion in the phase of the time series. Furthermore, the phase distortion is highly dependent on the corner period of the filter, and the distortion is relatively broadband. If the ground motion has much spectral content within several multiplicative factors of the corner period, then there should be significant differences when processed using causal filters with different corner periods. On the other hand, if the spectral content is limited to periods much less than the corner period, then the difference between causal and acausal filters should decrease with increasing corner periods of the filters.

The displacements resulting from the filtered accelerations are shown in Figures 2 and 3 for two stations that recorded the 1999 Hector Mine earthquake (the locations of the stations are given in Figure 4). The two figures are the same, except Figure 2 includes more of the time series to show the filter transients, while Figure 3 uses an expanded time scale to allow better comparison of the waveforms. For each figure the left column shows results for the causal filter, and the right for acausal filters. In applying the filters we followed the guidance of Converse and Brady (1992) in adding pre- and post-event pads of sufficient

length to allow for the filter response, starting at the first and last zero crossings of the recorded motions to avoid steps. The transient earthquake motion has subsided enough for padding with zeros after the event to be a reasonable procedure, and because pre-event motion is available, no assumptions are needed in adding pre-event zeros. Because on physical and observational grounds the earthquake motion is a transient with a finite duration, the acceleration time series is effectively known for as long a time as necessary to perform filtering, and there is no inconsistency in filtering at periods long compared to the finite duration of the recording (if in doubt about this, consider an accelerogram composed of a single cycle of a sine wave; that motion will have a step in displacement, but the accelerogram can be filtered at arbitrarily long periods by adding zeros as indicated). As expected, the causal filters produce no precursory filter transients, but the waveforms are quite dependent on the filter corner periods, particularly for the motion recorded at station 530. The waveforms from the acausal filters have just the opposite characteristics, with large precursory transients, but rather similar waveforms.

As a side note, the process of filtering and integration is independent of the order in which the operations are performed if adequate pads have been used. As a second side note, if the Butterworth filter is implemented in the time domain, the shape of the response in the frequency domain for the causal and acausal filters can never be the same: the causal and acausal filters will have amplitudes of $1/\sqrt{2}$ and $1/2$ at the corner frequency, respectively, regardless of the order of the filters (see the lower left panel in Figure 1).

<center>Effect of Filtering on Peak Acceleration, Velocity, and Displacement</center>

Tables 1 through 4 give peak motions for times series processed using a series of causal and acausal filters. The data came from stations HEC and 530 for the 1999 Hector Mine earthquake, station TCU068 for the 1999 Chi-Chi earthquake, and station RIN for the 1994 Northridge earthquake.

Acceleration, velocity, and displacement time series, as well as response spectra and ratios of response spectra are given in Figures 5 through 14 for the TCU068 and RIN recordings. (The jaggedness seen in the ratios has been confirmed in several ways: spectral values were computed at 200 periods between 1 and 6 sec, and the computations were repeated using the BAP software to do the padding, filtering, and response spectral computations.)

Looking at the tables and plots shows that the causally-filtered results show more variability than do those of the acausally filtered results. Particularly noticeable is the sensitivity of the peak accelerations to the filter corners for causal filters. In addition,

<center>– 3 –</center>

in general the longer-period motions seem to show a more systematic trend for acausally motions (for example, peak displacements in Table 1). Also worth noting are the differences in peak motions for the same filter period for the two types of filtering.

The ratios of spectra show that filter corners can influence the spectra for frequencies considerably smaller than the corner frequency of the filter (Figures 9 and 14). A rule of thumb that response spectra should not be used at frequencies greater than one-half the filter corner is suggested by the figures. This conclusion only applies to the low-order filters used here; for higher-order filters the response spectra could be used for frequencies closer to the filter frequencies (but I have not done a systematic study of this).

Effect on Response Spectra of Excluding Trailing Pads

All of the response spectra shown thus far were computed for records derived by filtering acceleration time series with both leading and trailing zero pads. What if the portion of the filtered record corresponding to the trailing pad was not included in the computation of response spectra (this is the case with the 1999-2003 data provided by the USGS, and as far as I know, all of the PEER data)? In other words, is it possible that the peak of the oscillator response in the time domain could occur after the end of the recorded portion of the motion? I experimented with this for the RIN recording, using the whole record and cutting off the record at the end of the recorded motion (the figure states this to be at a time of 170 sec, but the leading pad was 150 sec; the recording had a duration of only about 20 sec). The results, in Figure 15, suggest that for periods of engineering interest nothing is lost in the response spectra by ignoring the trailing pad.

Effect of Filtering on Inelastic Response Spectra

Figures 16 through 19 are taken from a paper by Boore and Akkar (2003); Figures 20 and 21, for RIN, are new to these notes. The figures show that the sensitivity to filter corners for causal filters is even more pronounced for inelastic spectra than for elastic spectra.

Acknowledgments

I thank Sinan Akkar for computing the inelastic spectra for station RIN.

References

Boore, D.M. and S. Akkar (2003). Effect of causal and acausal filters on elastic and inelastic response spectra, *Earthq. Eng. Struct. Dyn.* **32**, (in press).

Boore, D.M., C.D. Stephens, and W.B. Joyner (2002). Comments on baseline correction of digital strong-motion data: Examples from the 1999 Hector Mine, California, earthquake, *Bull. Seism. Soc. Am.* **92**, 1543–1560.

Converse, A.M. and A.G. Brady (1992). BAP — Basic strong-motion accelerogram processing software; Version 1.0, *U.S. Geol. Surv. Open-File Rept. 92-296A*, 174p.

Ji, C., D.J. Wald, and D.V. Helmberger (2002). Source description of the 1999 Hector Mine, California earthquake; Part II: Complexity of slip history, *Bull. Seism. Soc. Am.* **92**, 1208–1226.

```
              f_smc    flterl    pkmtn
   HP1C005A.SMC    0.005    322.9
   HP1C010A.SMC    0.010    324.0
   HP1C020A.SMC    0.020    326.2
   HP1C040A.SMC    0.040    330.9

   HP1A005A.SMC    0.005    321.8
   HP1A010A.SMC    0.010    321.8
   HP1A020A.SMC    0.020    321.8
   HP1A040A.SMC    0.040    321.8


   HP1C005V.SMC    0.005     43.9
   HP1C010V.SMC    0.010     43.8
   HP1C020V.SMC    0.020     43.3
   HP1C040V.SMC    0.040     41.6

   HP1A005V.SMC    0.005     44.1
   HP1A010V.SMC    0.010     44.2
   HP1A020V.SMC    0.020     44.4
   HP1A040V.SMC    0.040     44.4


   HP1C005D.SMC    0.005     11.5
   HP1C010D.SMC    0.010     10.4
   HP1C020D.SMC    0.020     11.8
   HP1C040D.SMC    0.040     12.7

   HP1A005D.SMC    0.005     16.2
   HP1A010D.SMC    0.010     14.1
   HP1A020D.SMC    0.020     12.7
   HP1A040D.SMC    0.040     12.0
```

Table 1. Acceleration, velocity, and displacement peak values, from headers of smc files of the EW motion at HEC from the 1999 Hector Mine earthquake, processed using causal and acausal filters. The file name indicates the station, type of filter, filter corner, and type of motion. For example, "`hp1c020v.smc`" is the velocity at HEC from a causal, 0.02 Hz filter, and "`hp1a040d.smc`" is the displacement from an acausal, 0.04 Hz filter. The data have been arranged in groups, with the accelerations, the velocities, and then the displacements, and within each group the causally filtered values are first.

f_smc	flterl	pkmtn
5P1C005A.SMC	0.005	51.7
5P1C010A.SMC	0.010	51.7
5P1C020A.SMC	0.020	51.5
5P1C040A.SMC	0.040	51.2
5P1A005A.SMC	0.005	51.9
5P1A010A.SMC	0.010	51.9
5P1A020A.SMC	0.020	51.9
5P1A040A.SMC	0.040	51.9
5P1C005V.SMC	0.005	5.3
5P1C010V.SMC	0.010	5.2
5P1C020V.SMC	0.020	4.7
5P1C040V.SMC	0.040	5.0
5P1A005V.SMC	0.005	5.2
5P1A010V.SMC	0.010	5.2
5P1A020V.SMC	0.020	5.2
5P1A040V.SMC	0.040	4.8
5P1C005D.SMC	0.005	6.3
5P1C010D.SMC	0.010	7.1
5P1C020D.SMC	0.020	6.6
5P1C040D.SMC	0.040	5.3
5P1A005D.SMC	0.005	5.2
5P1A010D.SMC	0.010	5.6
5P1A020D.SMC	0.020	5.5
5P1A040D.SMC	0.040	5.0

Table 2. Acceleration, velocity, and displacement peak values, from headers of smc files of the NS motion at 530 from the 1999 Hector Mine earthquake, processed using causal and acausal filters. The file name indicates the station, type of filter, filter corner, and type of motion. For example, "5p1c020v.smc" is the velocity at 530 from a causal, 0.02 Hz filter, and "5p1a040d.smc" is the displacement from an acausal, 0.04 Hz filter. The data have been arranged in groups, with the accelerations, the velocities, and then the displacements, and within each group the causally filtered values are first.

```
            f_smc   flterl    pkmtn
68NT100A.SMC     0.010    405.4
68NT050A.SMC     0.020    440.0
68NT025A.SMC     0.040    492.3
68NT012A.SMC     0.080    543.5


68PT100A.SMC     0.010    364.4
68PT050A.SMC     0.020    364.3
68PT025A.SMC     0.040    364.3
68PT012A.SMC     0.080    372.2


68NT100V.SMC     0.010    240.1
68NT050V.SMC     0.020    256.4
68NT025V.SMC     0.040    235.2
68NT012V.SMC     0.080    164.5


68PT100V.SMC     0.010    278.4
68PT050V.SMC     0.020    264.4
68PT025V.SMC     0.040    234.2
68PT012V.SMC     0.080    170.4


68NT100D.SMC     0.010    587.3
68NT050D.SMC     0.020    429.7
68NT025D.SMC     0.040    355.8
68NT012D.SMC     0.080    230.0


68PT100D.SMC     0.010    502.1
68PT050D.SMC     0.020    446.2
68PT025D.SMC     0.040    343.8
68PT012D.SMC     0.080    191.0
```

Table 3. Acceleration, velocity, and displacement peak values, from headers of smc files of the NS motion at TCU068 from the 1999 Chi-Chi earthquake, processed using causal and acausal filters. The file name indicates the station, type of filter, filter corner, and type of motion. For example, "68nt050v.smc" is the velocity from a causal, 50 sec filter, and "68pt025d.smc" is the displacement from an acausal, 25 sec filter (the "p" in the name stands for "padded", which is something needed for acausal filters). The data have been arranged in groups, with the accelerations, the velocities, and then the displacements, and within each group the causally filtered values are first.

f_smc	flter1	pkmtn
RINC010A.SMC	0.010	814.1
RINC020A.SMC	0.020	810.1
RINC040A.SMC	0.040	821.8
RINC080A.SMC	0.080	884.6
RINC160A.SMC	0.160	963.6
RINA010A.SMC	0.010	817.0
RINA020A.SMC	0.020	817.1
RINA040A.SMC	0.040	817.4
RINA080A.SMC	0.080	817.7
RINA160A.SMC	0.160	815.8
RINC010V.SMC	0.010	167.5
RINC020V.SMC	0.020	164.3
RINC040V.SMC	0.040	157.1
RINC080V.SMC	0.080	141.1
RINC160V.SMC	0.160	135.2
RINA010V.SMC	0.010	168.4
RINA020V.SMC	0.020	166.9
RINA040V.SMC	0.040	165.2
RINA080V.SMC	0.080	162.2
RINA160V.SMC	0.160	155.2
RINC010D.SMC	0.010	43.8
RINC020D.SMC	0.020	43.9
RINC040D.SMC	0.040	43.7
RINC080D.SMC	0.080	41.5
RINC160D.SMC	0.160	34.2
RINA010D.SMC	0.010	55.0
RINA020D.SMC	0.020	45.3
RINA040D.SMC	0.040	35.3
RINA080D.SMC	0.080	29.1
RINA160D.SMC	0.160	25.2

Table 4. Acceleration, velocity, and displacement peak values, from headers of smc files of the 228 degree motion at RIN from the 1994 Northridge earthquake, processed using causal and acausal filters. The file name indicates the station, type of filter, filter corner, and type of motion. For example, "rinc020v.smc" is the velocity from a causal, 0.02 Hz filter, and "rina040d.smc" is the displacement from an acausal, 0.04 Hz filter. The data have been arranged in groups, with the accelerations, the velocities, and then the displacements, and within each group the causally filtered values are first.
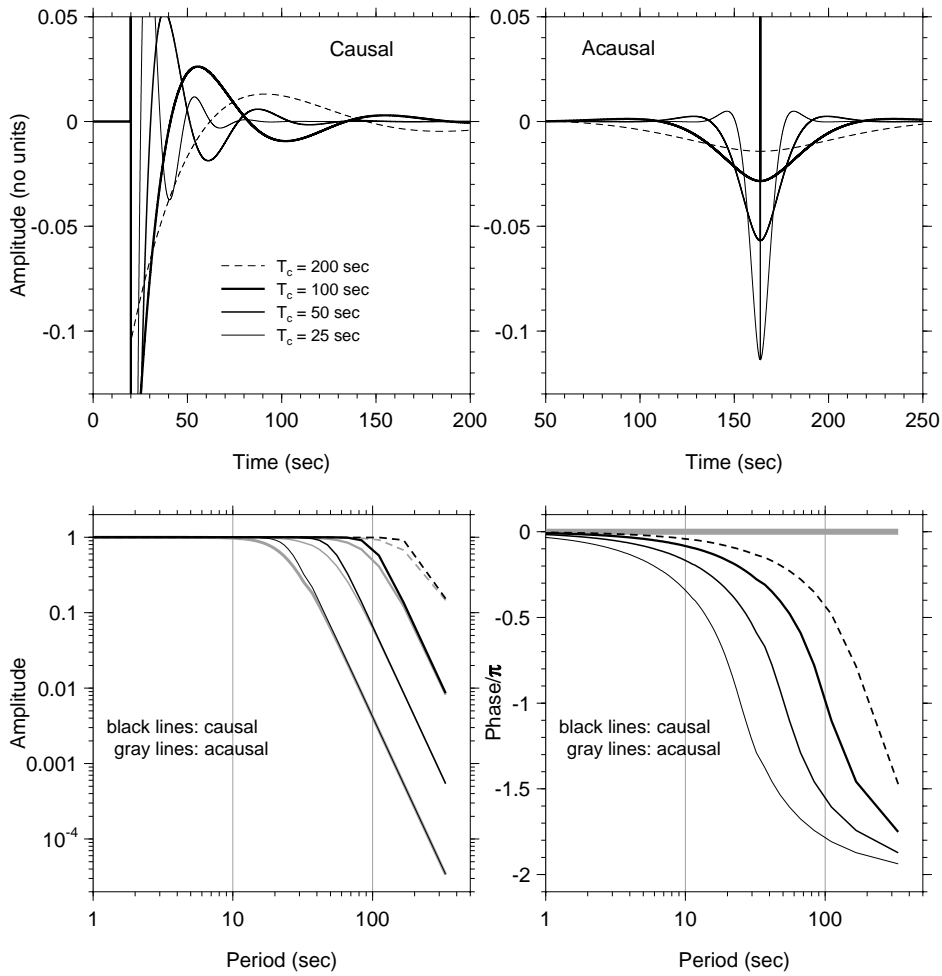
Figure 1. Results of filtering an impulse with amplitude of 256 with both causal and acausal filters, with corner periods of 200, 100, 50, and 25 sec. The time-domain responses as well as the Fourier amplitude and phase spectra are shown (the Fourier spectra were computed by taking the FFT of the time-domain spike, using program ampph4lc.for; the results agree with the theoretical results). The time series for the causal filters have been shifted to the left, compared to the location of the responses for the acausal filters, in order to capture most of the tails of the responses. Note that the time-domain impulse responses shown in the top row are plotted at a greatly expanded scale to show details; the responses are actually dominated by impulses of amplitude 256. The legend for corner periods (T_c) shown in the upper left plot is the same for all plots. The plots of the amplitude and phase responses combine both the causal and acausal filter responses; the acausal responses are plotted using gray lines. The phase spectra have been corrected for the linear phase due to placing the impulse at a time not equal to 0.0, and the corrected phase spectra have been normalized by dividing by π. Note the large phase shifts for the causal filters, even for periods away from the corner periods, and the difference in the phase shifts for the different filters. In contrast, the phase shifts for the acausal filters are zero. (From Boore and Akkar, 2003.)
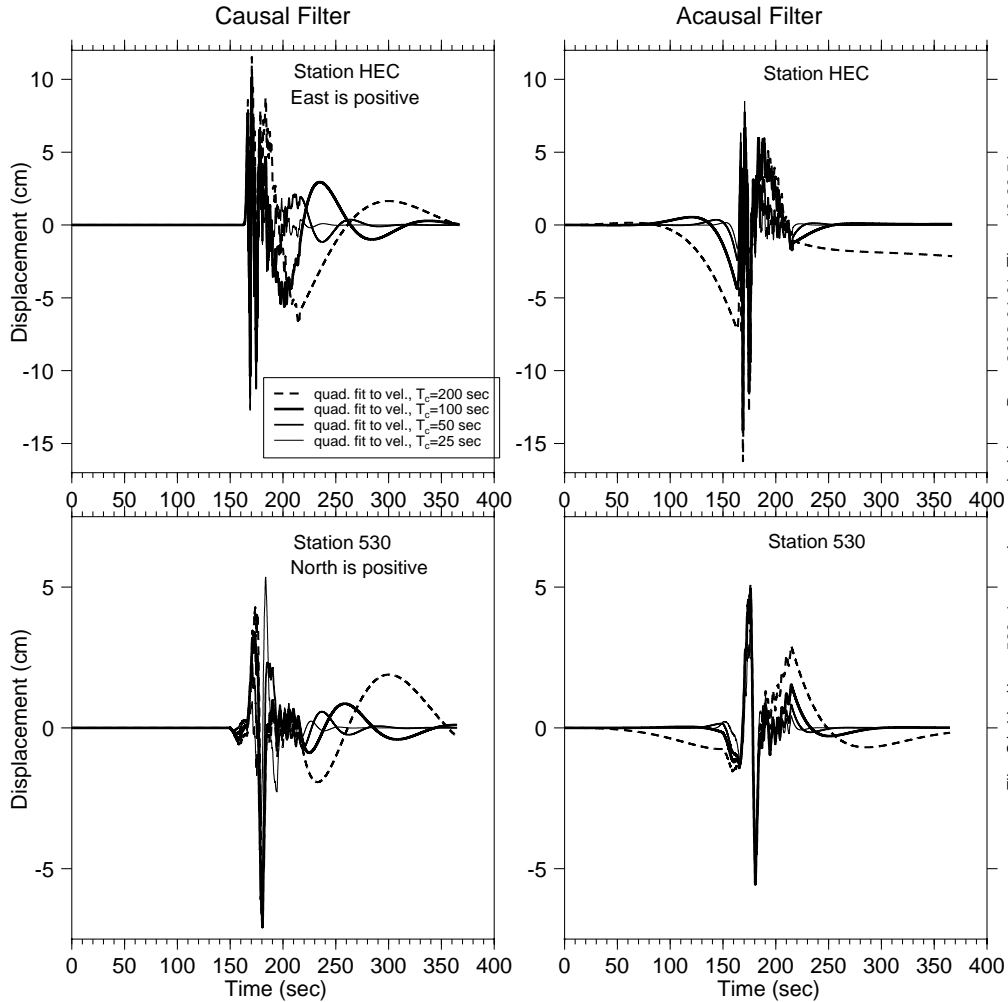
Figure 2. Displacements obtained by integrating accelerograms processed with a series of causal and acausal filters for both stations HEC and 530. The left hand and right hand columns contain results from records processed using causal and acausal filters, respectively. The legend relating the line type to the corner period of the filter is the same for all plots. The causal filters are 4th order Butterworth filters, and the acausal filters are produced by passing the time series in opposite directions through two 2nd order Butterworth filters (so that the roll-off at long periods is the same for both filters). Pre-event zero pads have been added to the accelerations at both stations, although this was necessary only for the acausally filtered data. (Modified from Boore and Akkar, 2003 to show the whole padded time series.)
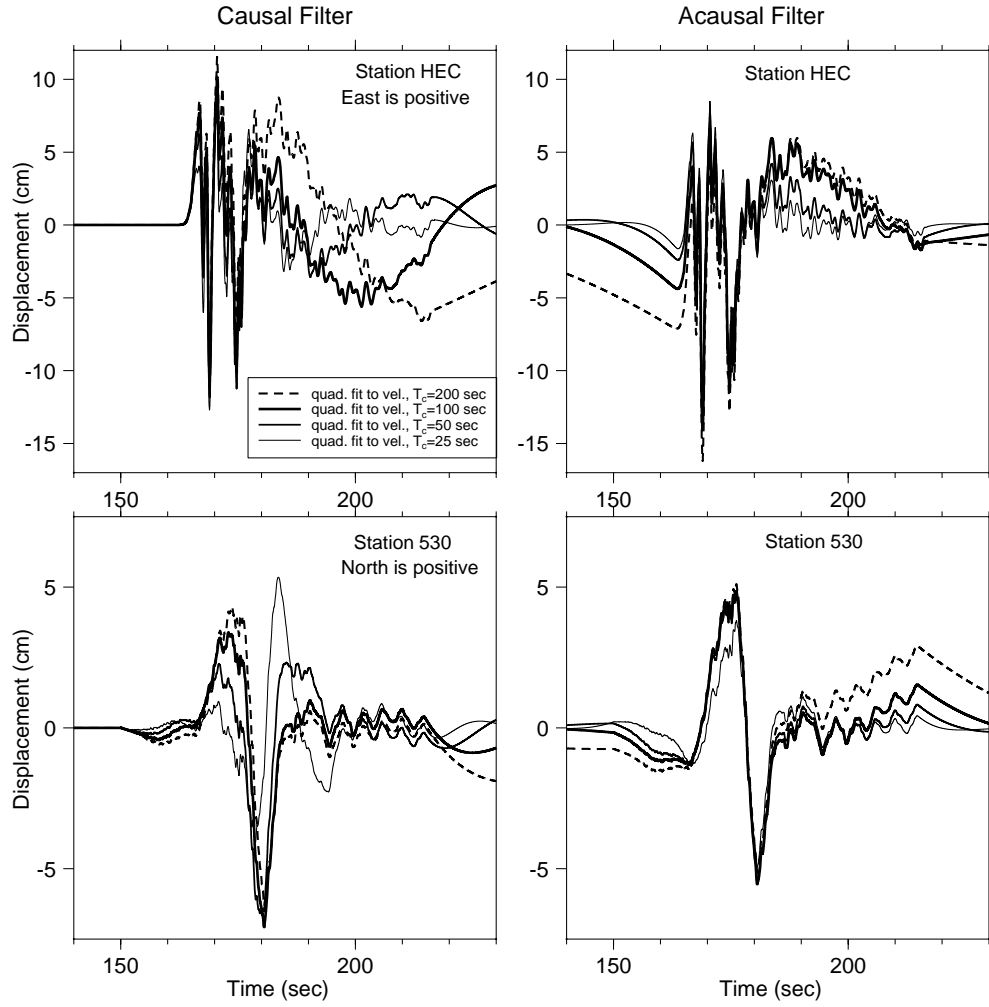
Figure 3. The same as Figure 2, but at an expanded time scale. (From Boore and Akkar, 2003.)
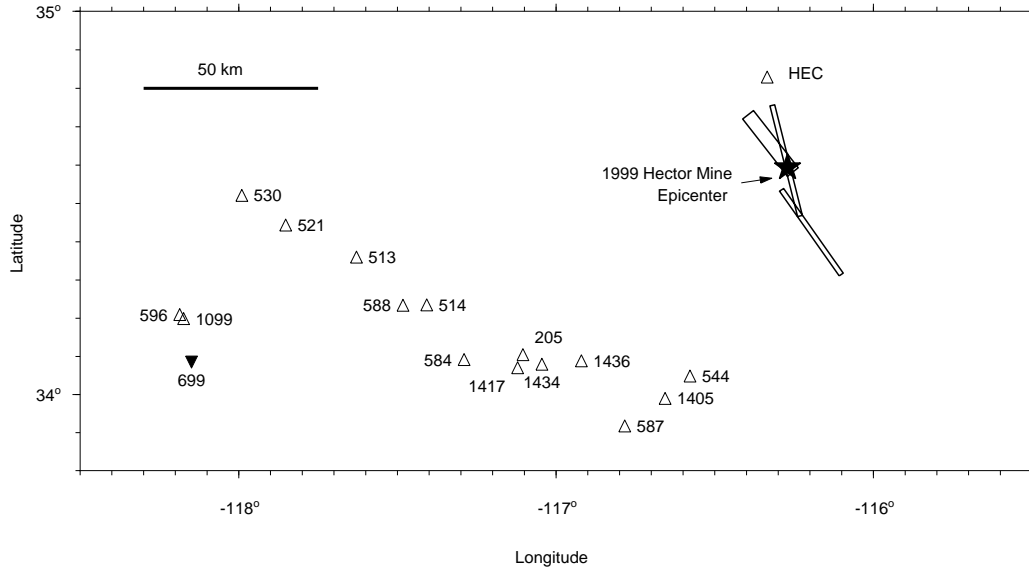
Figure 4. Map showing some of the stations that recorded the 1999 Hector Mine earthquake. Records from stations labeled 530 and HEC were used in this paper. The three rectangles near the epicenter are the surface projections of the fault planes used in Ji *et al.*'s (2002) fault model; the epicenter is shown by the star. The numerical labels are the serial numbers of the recorders at the stations; these numbers are used in naming the data files provided by the USGS. The official NSMP station numbers are different, but they have not been used to avoid confusion in relating a station shown on the map with the data file for the time series recorded at that station. Records from all stations shown here were digitally recorded. The records from station 530 were digitized using about 4280 counts/cm/s^2; those from station HEC were digitized at 2140 counts/cm/s^2. The sensors at all stations are force-balance accelerometers with natural frequency greater than 50 Hz. The data from TriNet station HEC were obtained through the Southern California Earthquake Data Center (SCEDC); the data from station 530 are from the National Strong-Motion Program (NSMP) of the U.S. Geological Survey (http://nsmp.wr.usgs.gov). (This figure is adapted from Boore *et al.*, 2002.)
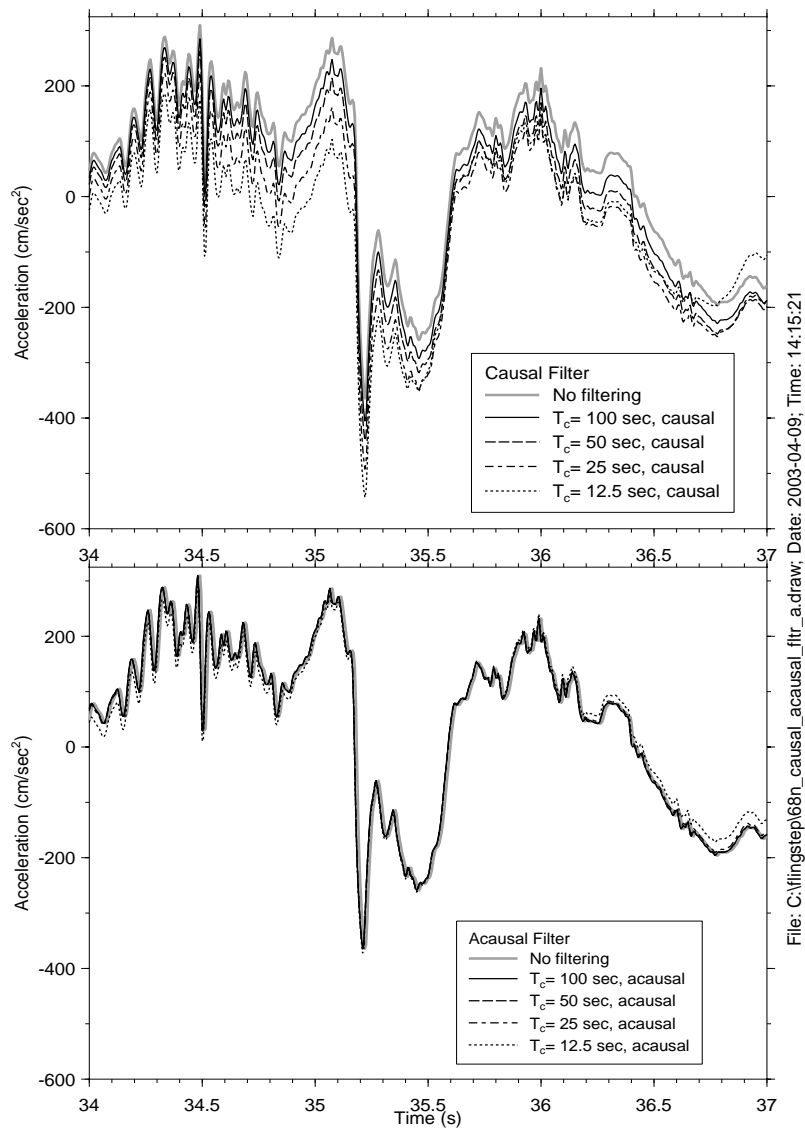
Figure 5. Accelerations from the NS component of the recording at TCU068 during the 1999 Chi-Chi earthquake at an expanded time scale for causal (top figure) and acausal (bottom figure) filtering.
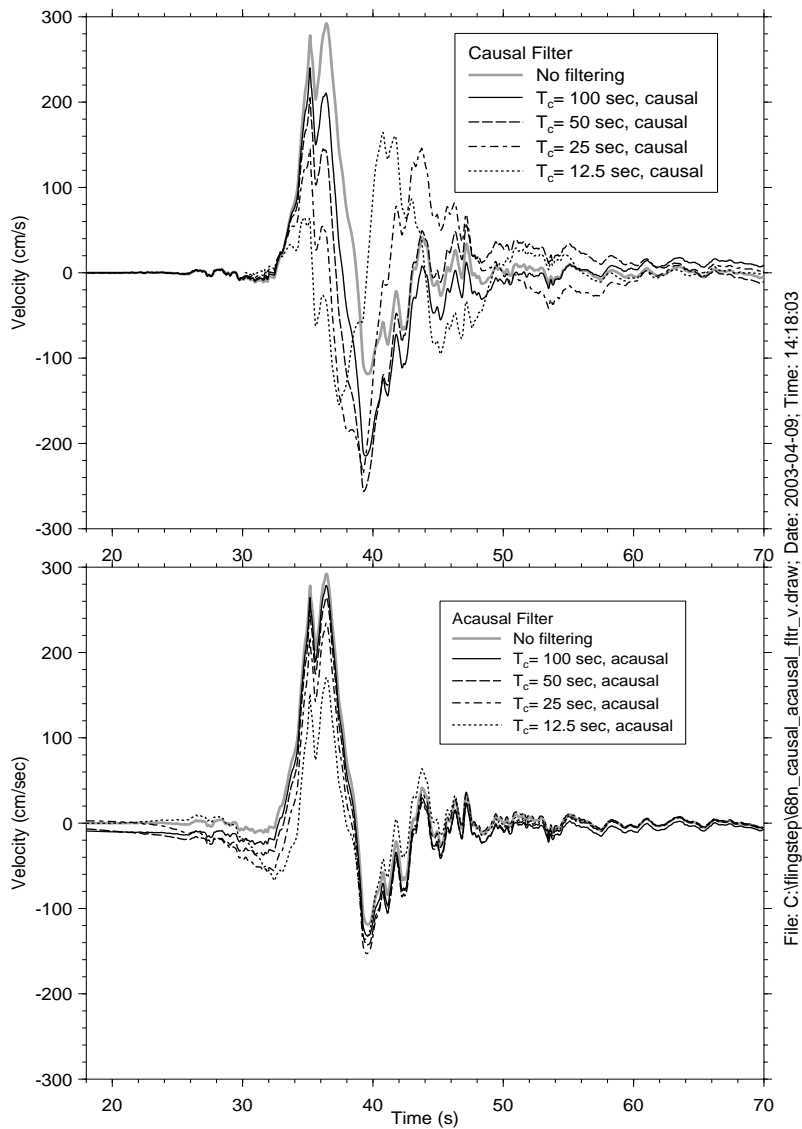
Figure 6. Velocities from the NS component of the recording at TCU068 during the 1999 Chi-Chi earthquake for causal (top figure) and acausal (bottom figure) filtering for a portion of the padded time series.
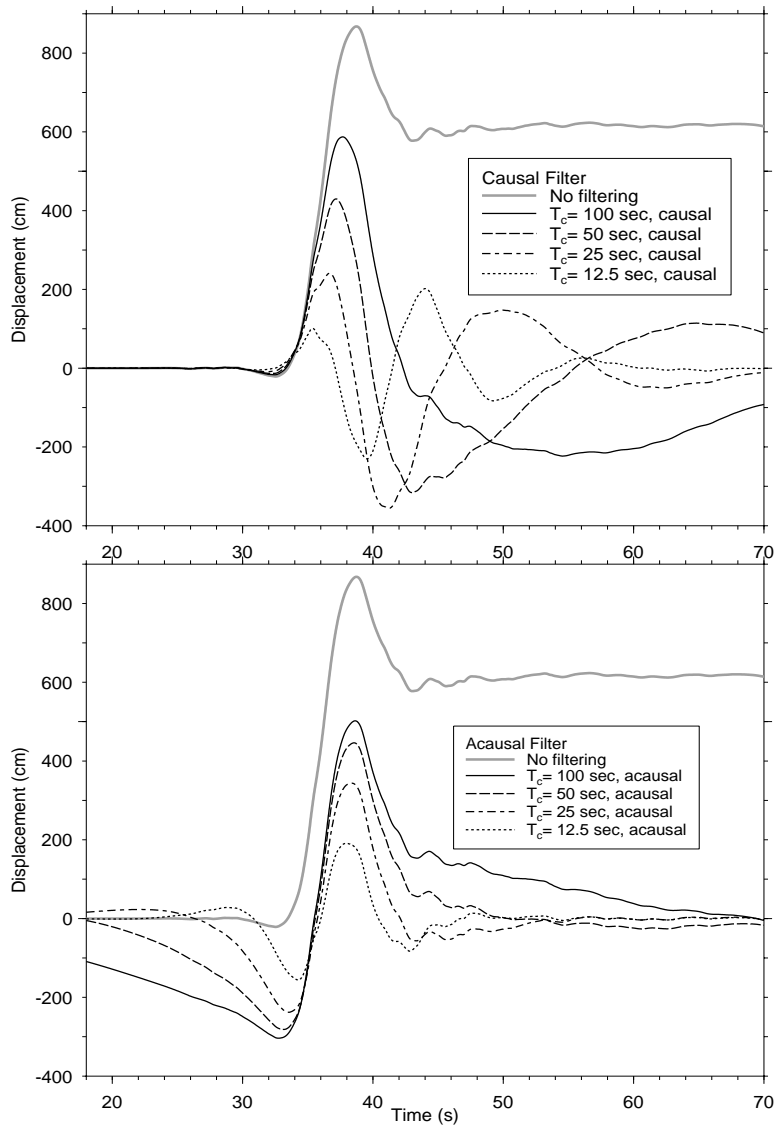
Figure 7. Displacements from the NS component of the recording at TCU068 during the 1999 Chi-Chi earthquake for causal (top figure) and acausal (bottom figure) filtering for a portion of the padded time series.
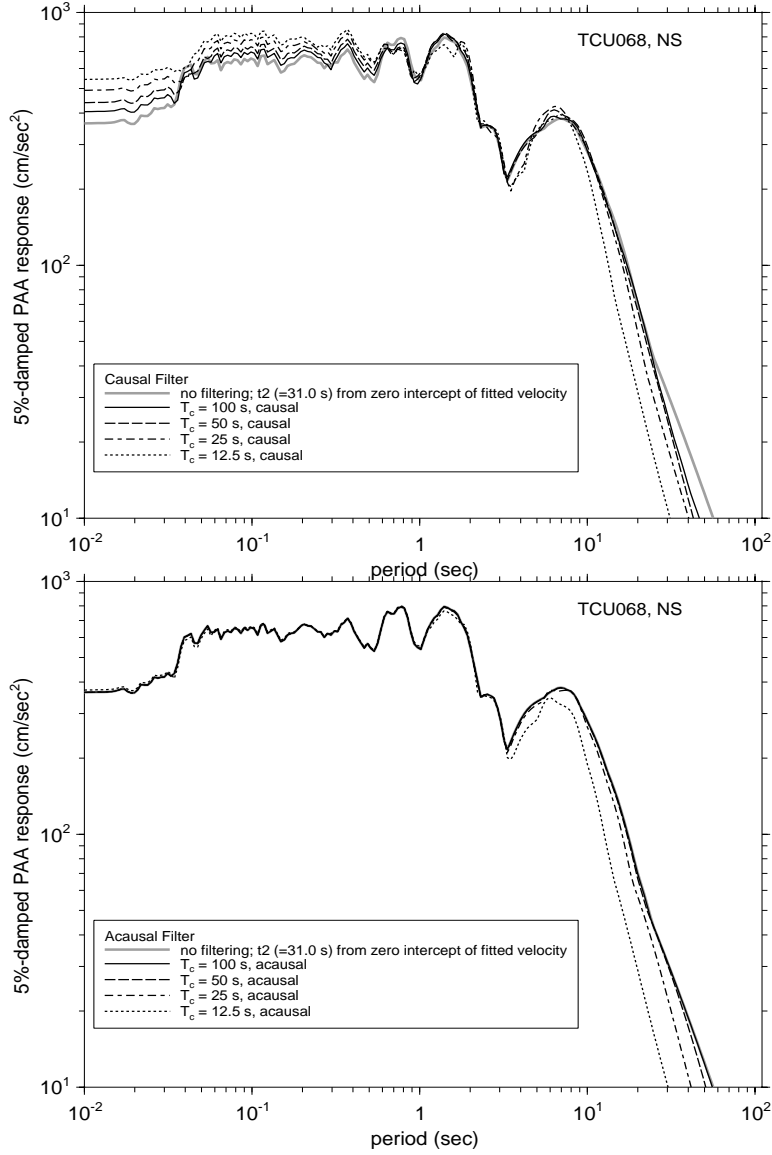
Figure 8. 5%-damped pseudo absolute acceleration spectra (in cm/s/s) from the NS component of the recording at TCU068 during the 1999 Chi-Chi earthquake for causal (top figure) and acausal (bottom figure) filtering.
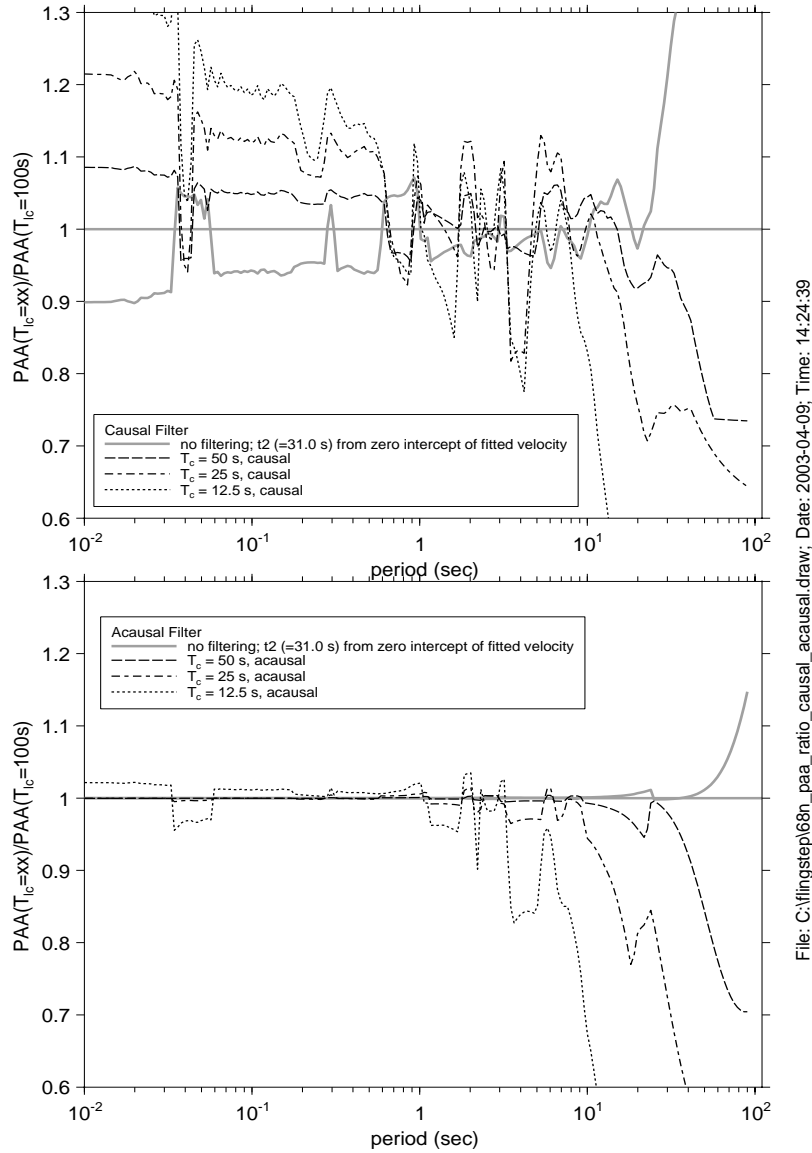
Figure 9. Ratio of 5%-damped pseudo absolute acceleration spectra (in cm/s/s) from the NS component of the recording at TCU068 during the 1999 Chi-Chi earthquake for causal (top figure) and acausal (bottom figure) filtering, using the results for a filter corner of 100 sec as reference.
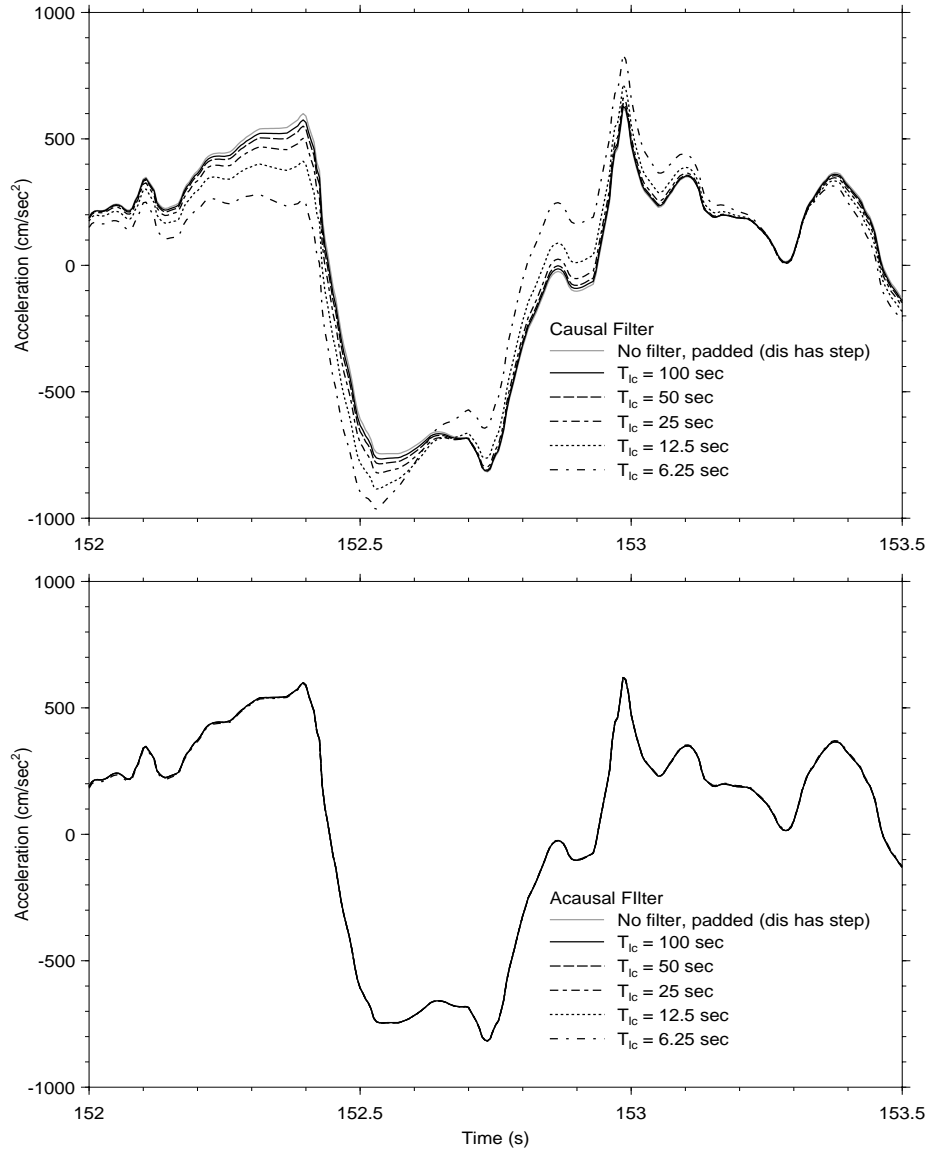
Figure 10. Accelerations from the 228 degree component of the recording at Rinaldi during the 1994 Northridge earthquake at an expanded time scale for causal (top figure) and acausal (bottom figure) filtering.
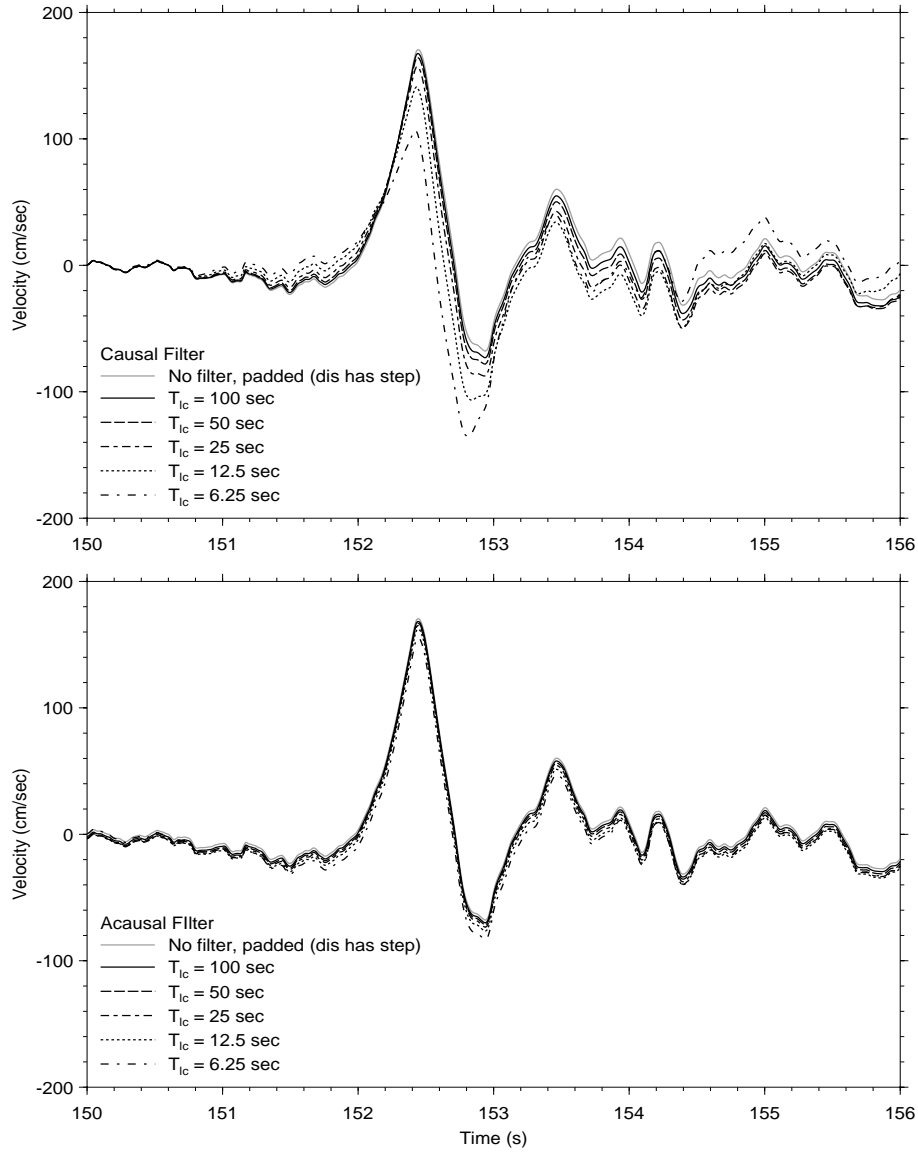
Figure 11. Velocities from the 228 degree component of the recording at Rinaldi during the 1994 Northridge earthquake at an expanded time scale for causal (top figure) and acausal (bottom figure) filtering.
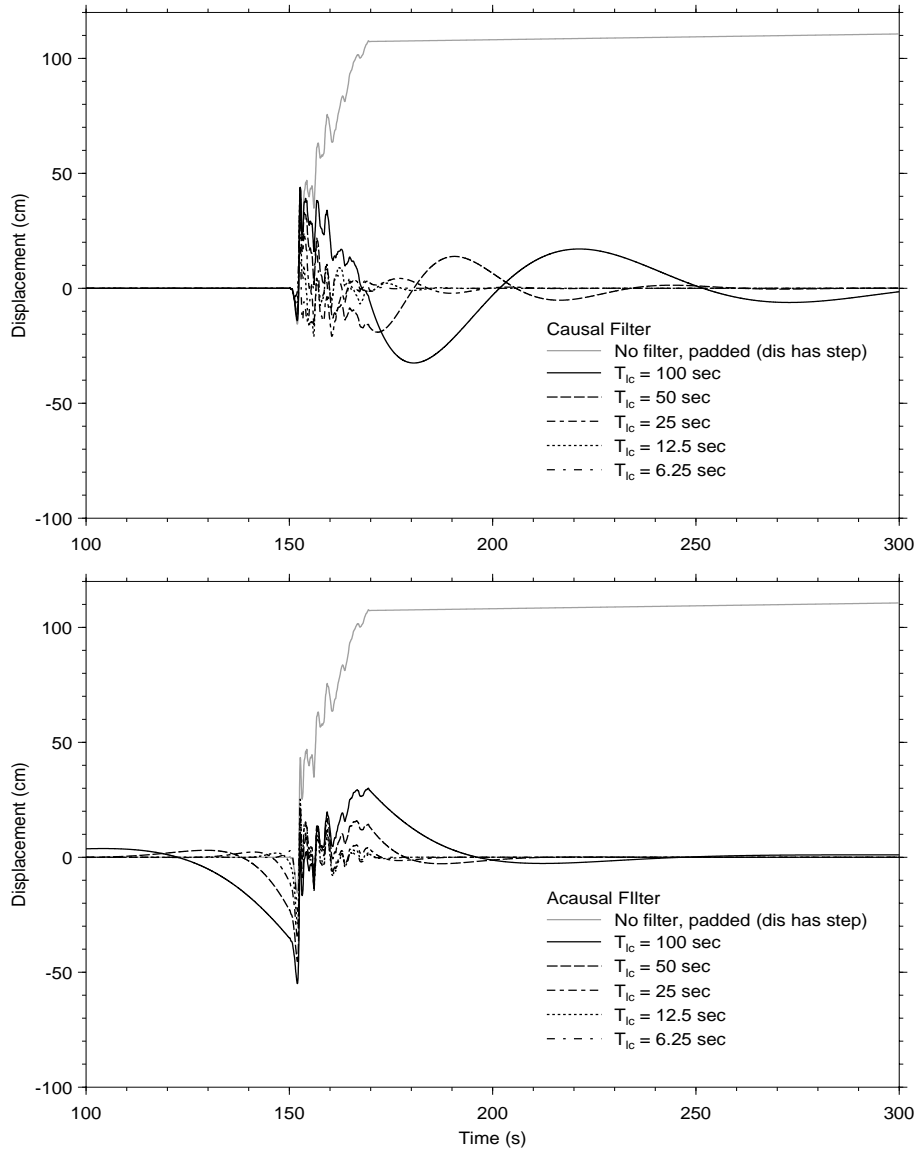
Figure 12. Displacements from the 228 degree component of the recording at Rinaldi during the 1994 Northridge earthquake at an expanded time scale for causal (top figure) and acausal (bottom figure) filtering.
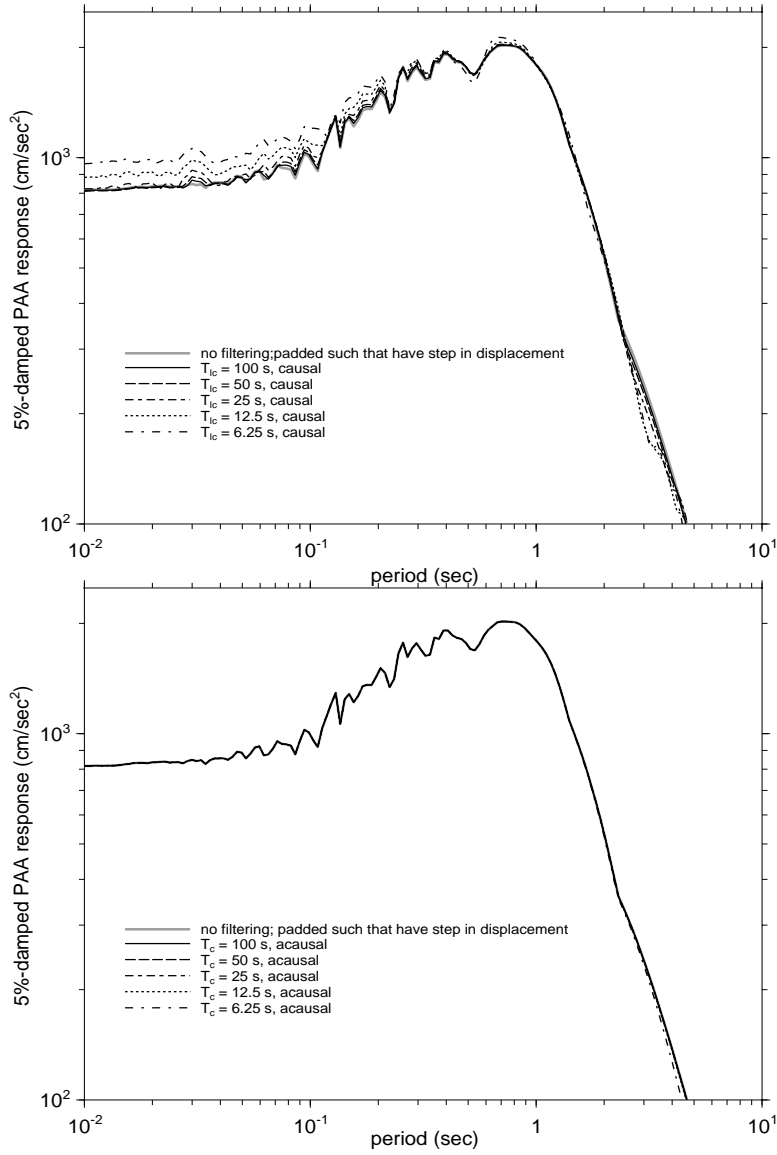
Figure 13. 5%-damped pseudo absolute acceleration spectra (in cm/s/s) from the 228 degree component of the recording at Rinaldi during the 1994 Northridge earthquake for causal (top figure) and acausal (bottom figure) filtering.
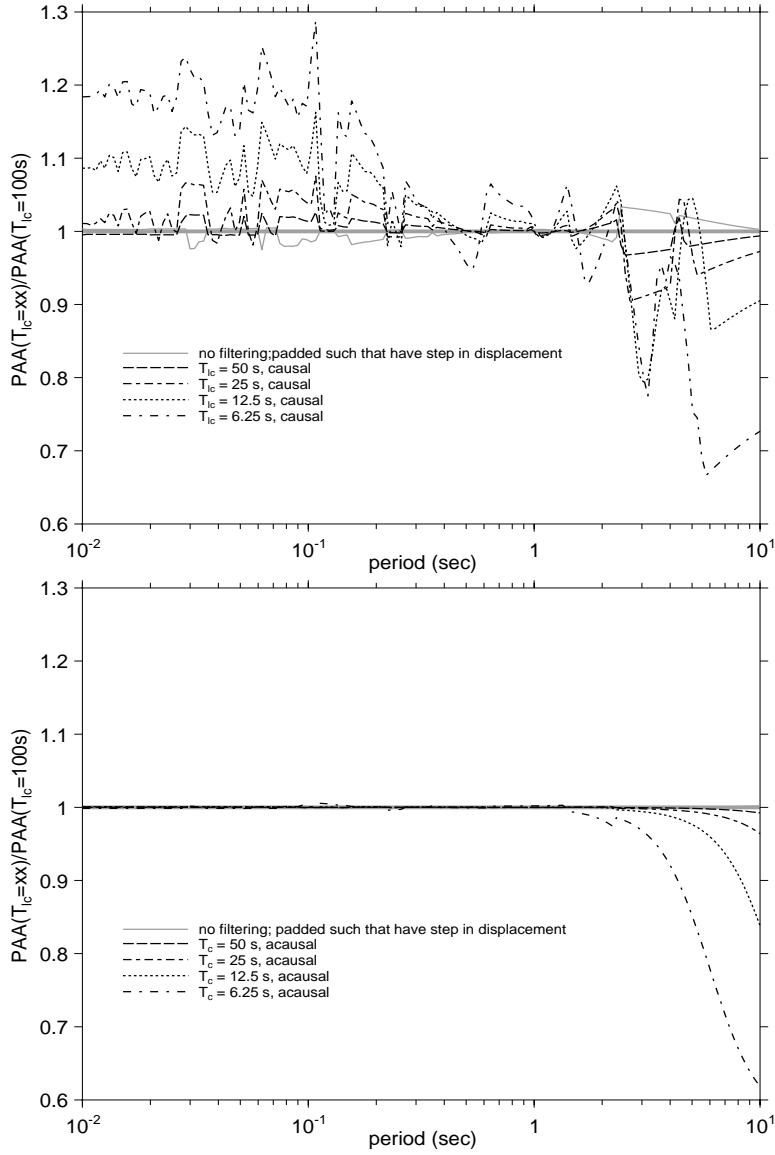
Figure 14. Ratio of 5%-damped pseudo absolute acceleration spectra (in cm/s/s) from the 228 degree component of the recording at Rinaldi during the 1994 Northridge earthquake for causal (top figure) and acausal (bottom figure) filtering, using the results for a filter corner of 100 sec as reference.
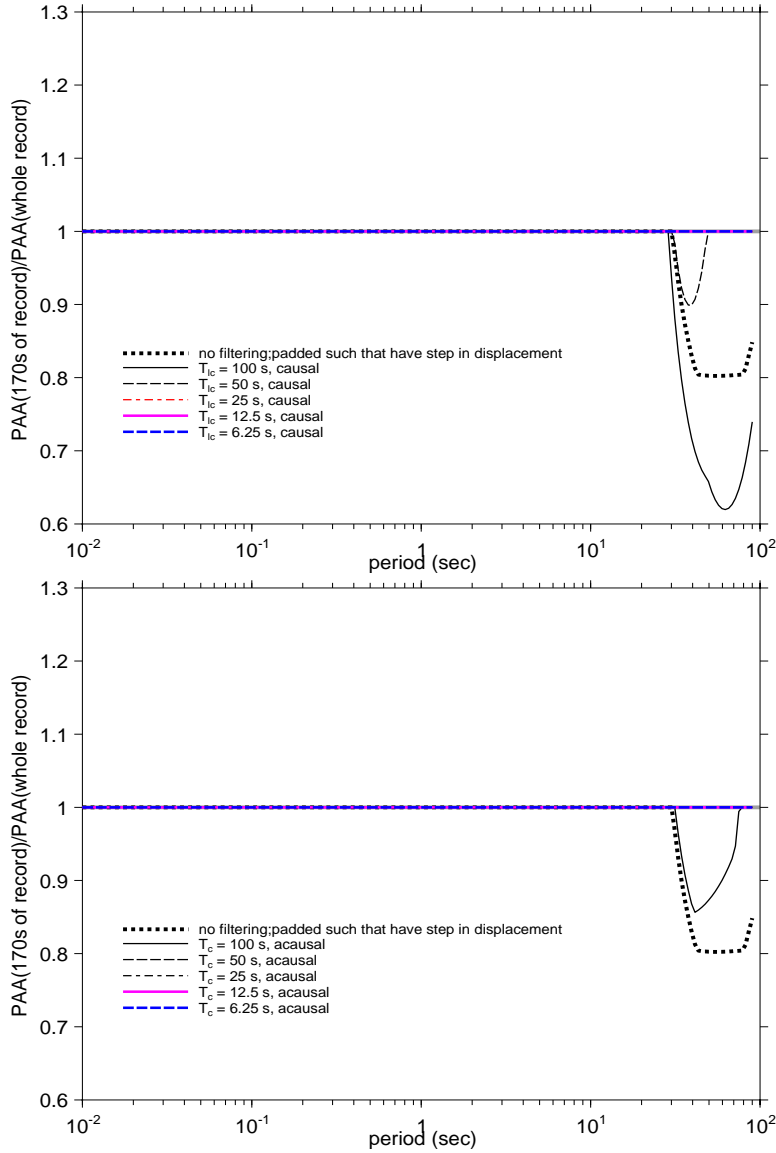
Figure 15. Ratio of 5%-damped pseudo absolute acceleration spectra (in cm/s/s) from the 228 degree component of the recording at Rinaldi during the 1994 Northridge earthquake for causal (top figure) and acausal (bottom figure) filtering, with and without the filter transients produced by continuing the filters into the trailing zero-padded portion of the unfiltered acceleration record. Note that the ratio here is of spectra computed for different lengths of the same record, not different records (as in the previous figure).

HEC: Causal Filters

HEC: Acausal Filters

Elastic Response

Elastic Response

T_c = 200 sec
T_c = 100 sec
T_c = 50 sec
T_c = 25 sec

5%-damped Displacement Response (cm)

Inelastic response (R=3)

Inelastic response (R=3)

Period (sec)

Period (sec)
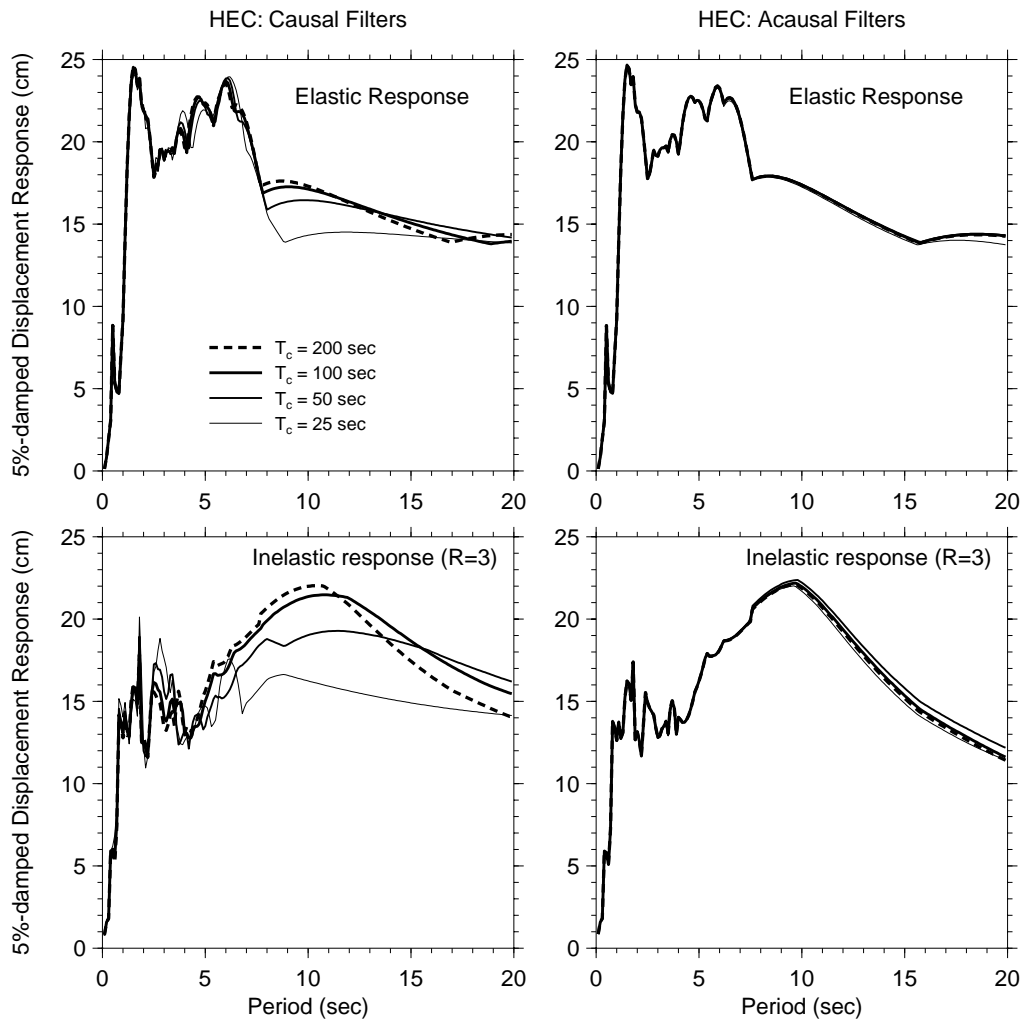
Figure 16.   Elastic and inelastic 5%-damped displacement response spectra for the recordings at station HEC, filtered using causal and acausal filters. The dashed line (for a corner period of 200 sec) was the reference spectra for the ratios shown in the next figure. (From Boore and Akkar, 2003.)
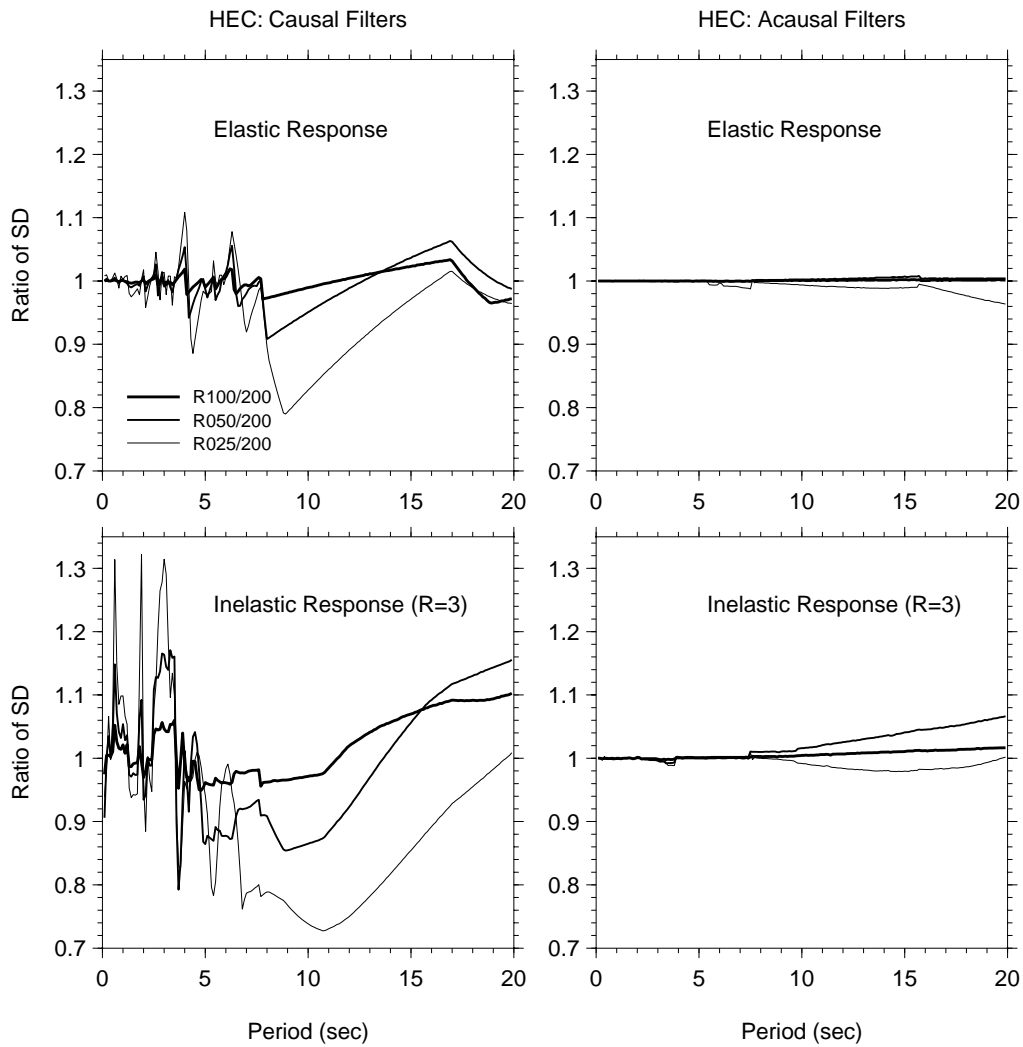
Figure 17. Ratios of response spectra for station HEC. The legend for the ratios is somewhat cryptic, but it should be clear that "R025/200" means that the response spectrum obtained from the acceleration time series filtered with a corner period of 25 sec was divided by the response spectrum from the acceleration time series filtered with a corner period of 200 sec. (From Boore and Akkar, 2003.)
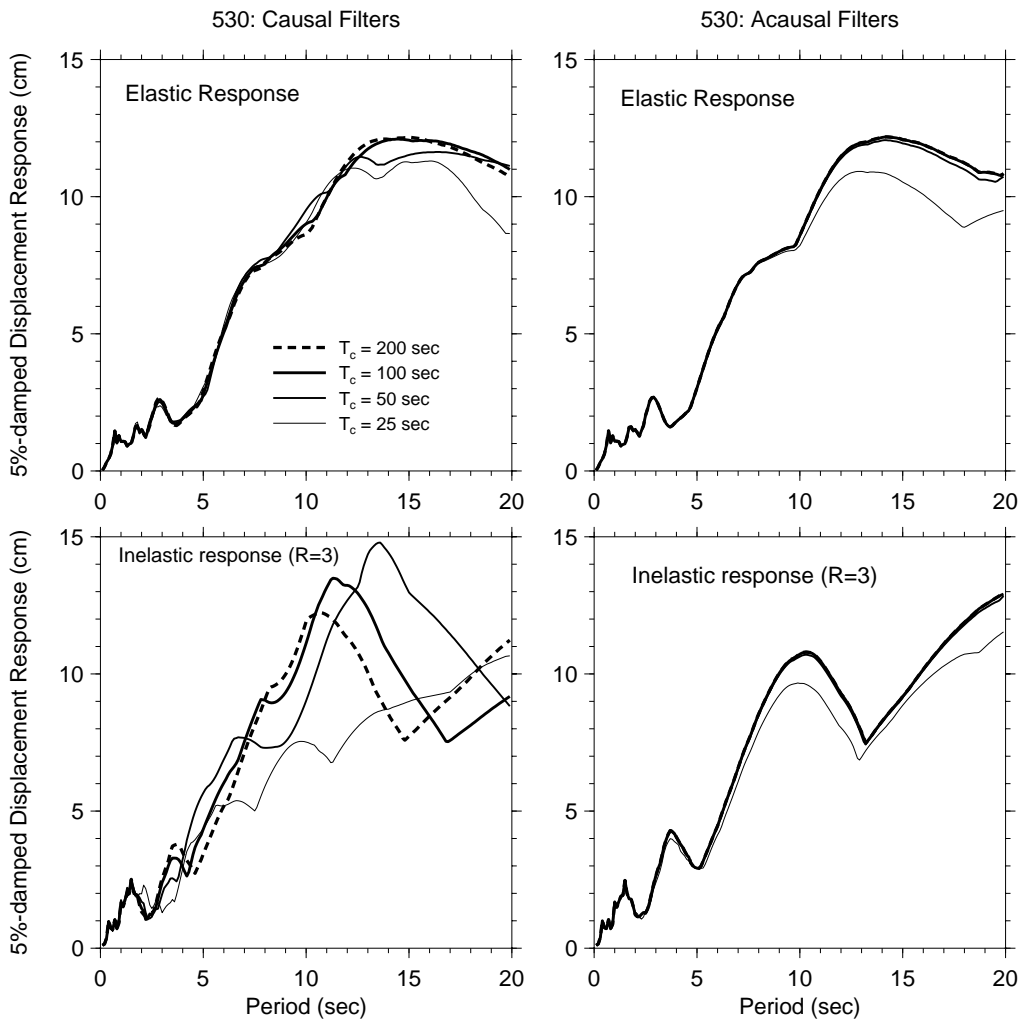
Figure 18. Elastic and inelastic 5%-damped displacement response spectra for the recordings at station 530, filtered using causal and acausal filters. The dashed line (for a corner period period of 200 sec) was the reference spectra for the ratios shown in the next figure. (From Boore and Akkar, 2003.)
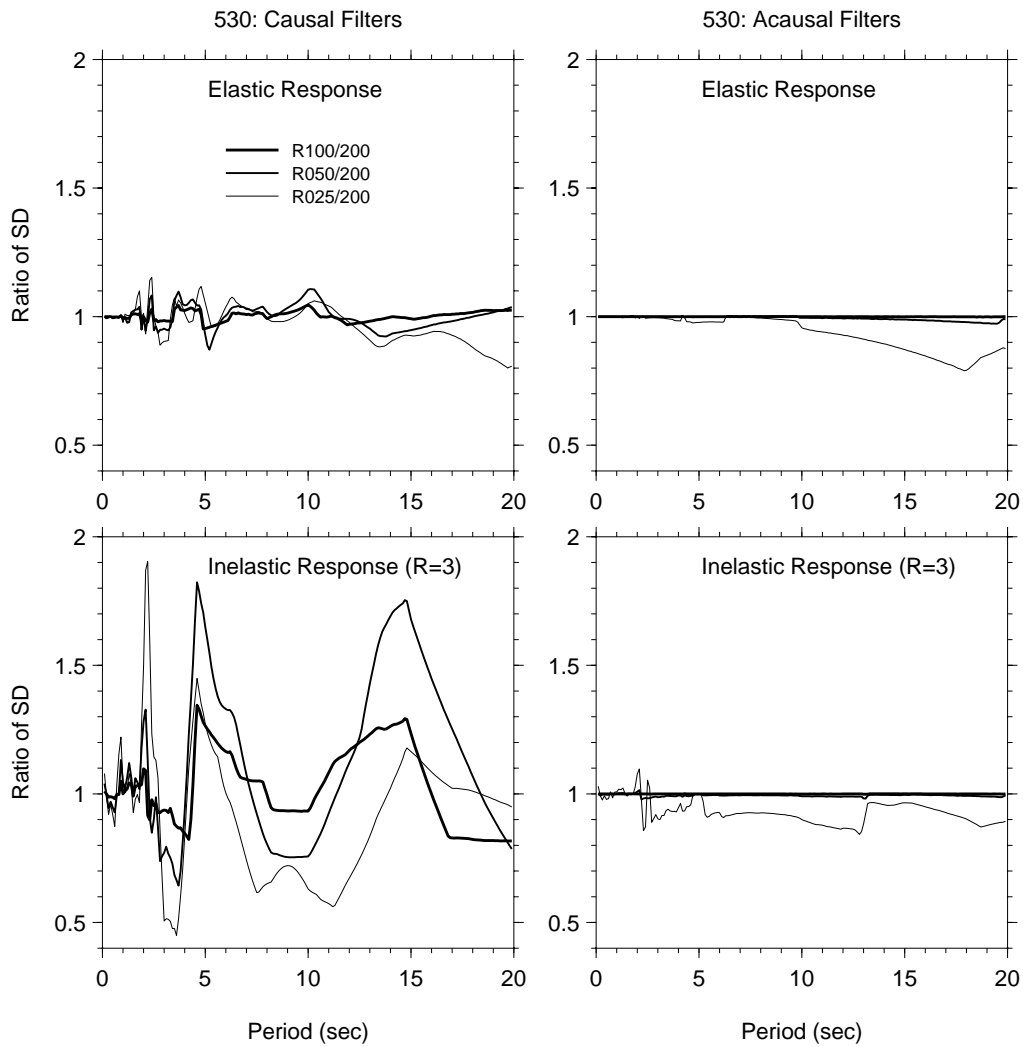
Figure 19. Ratios of response spectra for station 530. The legend for the ratios is somewhat cryptic, but it should be clear that "R025/200" means that the response spectrum obtained from the acceleration time series filtered with a corner period of 25 sec was divided by the response spectrum from the acceleration time series filtered with a corner period of 200 sec. (From Boore and Akkar, 2003.)
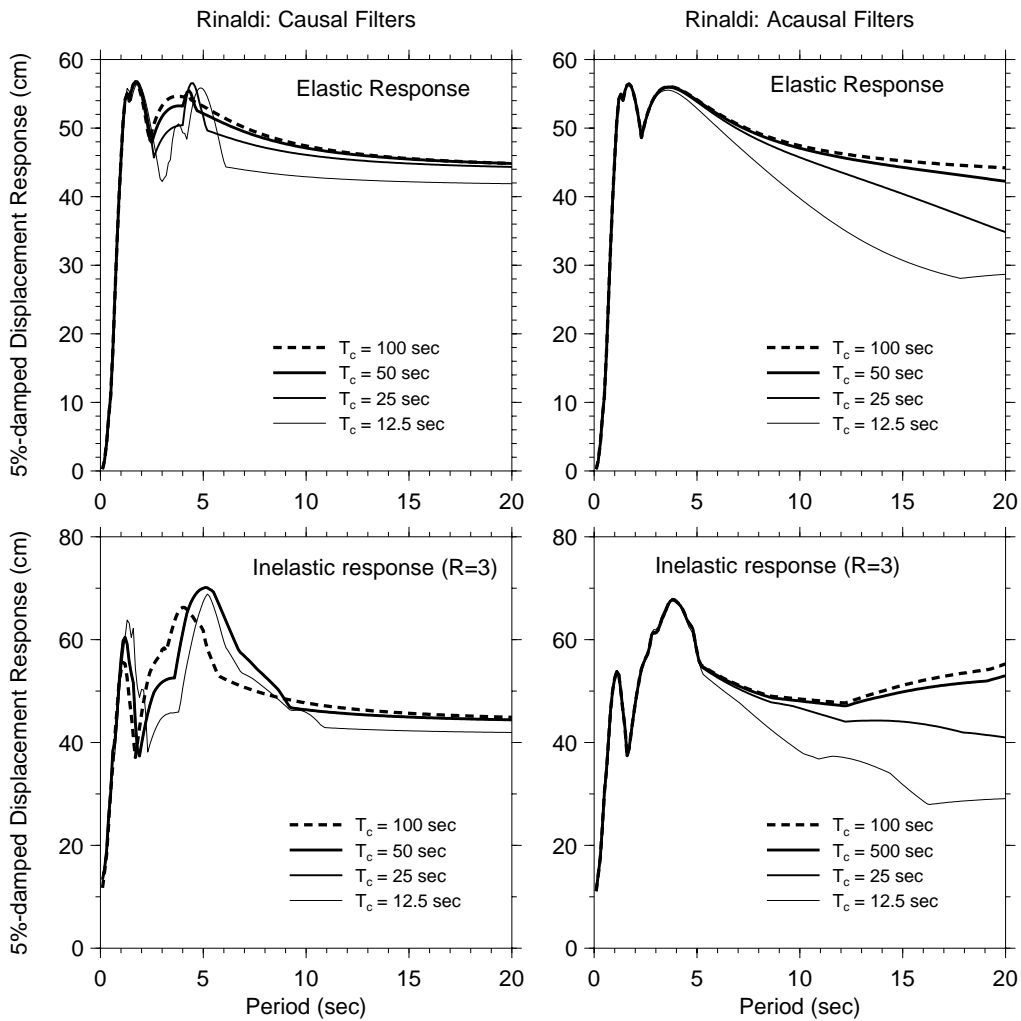
Figure 20.   Elastic and inelastic 5%-damped displacement response spectra for the recordings at station Rinaldi, filtered using causal and acausal filters. The dashed line (for a corner period period of 100 sec) was the reference spectra for the ratios shown in the next figure.
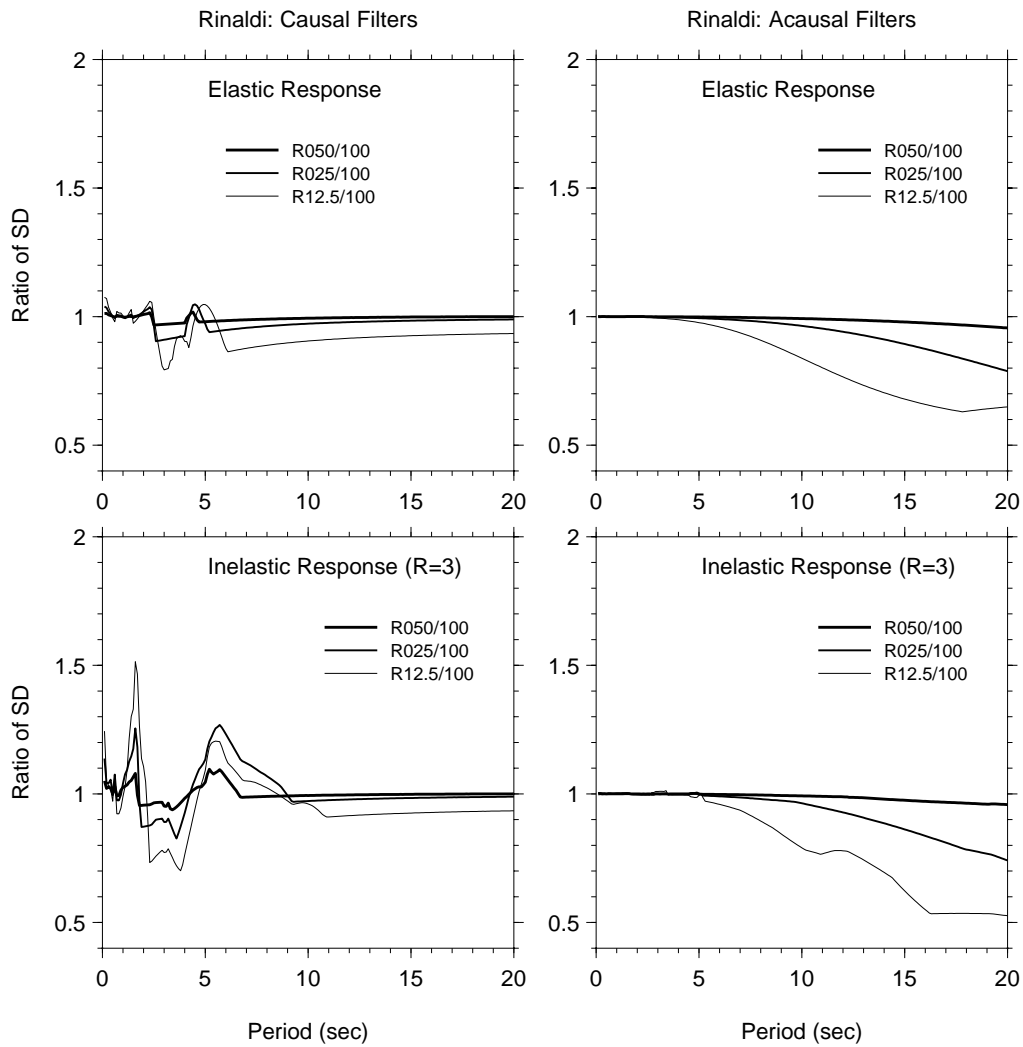
Figure 21. Ratios of response spectra for station Rinaldi. The legend for the ratios is somewhat cryptic, but it should be clear that "R025/100" means that the response spectrum obtained from the acceleration time series filtered with a corner period of 25 sec was divided by the response spectrum from the acceleration time series filtered with a corner period of 100 sec.